



## Research article

## Dependence on temperature and pressure of second cumulant and correlation effects during EXAFS in intermetallic alloys



Nguyen Ba Duc\*

Faculty of Physics, Tan Trao University, Tuyen Quang, Viet Nam

## ARTICLE INFO

## Keywords:

Non-harmonic  
Correlated function  
MSD  
Second cumulants  
DWF

## ABSTRACT

The present article is aimed to investigate the second cumulants, and the thermodynamic quantities are dependent on temperature and pressure in the X-ray absorption fine structure spectrum. The expressions have been built by using the model of the non-harmonic correlation of Einstein and Debye. A simple calculation was used to instead complex problems caused by the interaction of many particles in the system. The significant results of this work are the Morse potential parameters have been theoretically calculated method, determined the temperature dependence of the second cumulant, mean square displacement and correlation function for copper, tungsten, and copper-tungsten alloy of ratio 93-07 percent ( $W_{93}Cu_{07}$ ) under pressure up to 14GPa. Calculated the second cumulant dependence on the pressure in a range from 0GPa to 14GPa and clearly analysed the difference between the second cumulant at different pressure for atoms of tungsten, copper and tungsten-copper alloy. Numerical results according to the present theory agree well with experimental data and previous views.

## 1. Introduction

The Debye-Waller factor (DWF) appear in Extended X-Ray Absorption Fine Structure (EXAFS) were determined in previous researches [2, 5], as the temperature increases, DWF causes a decrease in the amplitude of the EXAFS spectrum due to thermal oscillations of the atoms, DWF decreases exponentially, in which a quantity is the second cumulant  $\sigma^2(T)$  or the Mean Square Relative Displacement (MSRD) of the pair atoms. MSRD mentions correlated averages of the relative displacement for a pair of atoms. In an inversion, in the diffraction or X-ray absorption, the DWF has form  $u^2(T)$  characteristic for an atom's Mean Square Displacement (MSD) [1]. The quantities  $\sigma^2(T)$  and  $u^2(T)$  are related to each other, from which it can deduce Displacement-Displacement Correlation Function  $C_R(T)$  to define the correlated influences in the atoms oscillation. DWF is a quantity used mainly to determine the crystal structure and thermodynamic parameters in the EXAFS spectrum. There have been many studies on calculating and analyzing the temperature dependence of the second cumulant or MSRD. [11, 14], MSD  $u^2(T)$  [5, 13], and the correlation effects between thermodynamic parameters for cubic crystal structures [6]. However, the temperature dependence under pressure affects up to 14GPa of second cumulant  $\sigma^2(T)$ , mean square displacement  $u^2(T)$ , atomic correlation displacement functions  $C_R(T)$  and the relationship between thermodynamic parameters due to anharmonicity in

EXAFS spectra for intermetallic alloys have not been studied to date. In previous studies, the thermodynamic parameters and the cumulants or DWF were determined depending only on temperature or pressure. This study considered the effects of both temperature and pressure for thermodynamic parameters of crystals because thermodynamic parameters, the second cumulant or MSRD and MSD, are also very sensitive to pressure. If these effects are fully understood, creating new materials that can withstand high temperatures and withstand the effects of high pressure will be a new step in materials science.

In this work, the dependence on temperature of the correlation displacement function with the force of pressure is analyzed and described based on the Debye-Waller coefficient or the second cumulant in EXAFS. Using the anharmonic correlation Einstein model (ACEM) [6], have been determined the expression of the second cumulant depends on temperature under the influence of pressure  $\sigma^2(T; P)$ . By the anharmonic correlation Debye model (ACDM) [7], we defined the mean square displacement  $u^2(T; P)$  and the relationship between thermodynamic parameters due to the non-harmonicity in EXAFS. The complex three-dimensional problem due to the many-particle effect was replaced by a one-dimensional problem based on effective potentials, in which have calculated the interactions of the absorbed and scattered atoms with the neighbouring atoms. The Morse potential describes single-pair interactions of atoms. This work also compares the second cumulant  $\sigma^2$

\* Corresponding author.

E-mail address: [ducnb@daihoctantrao.edu.vn](mailto:ducnb@daihoctantrao.edu.vn).

obtained from ACEM and the mean square displacement  $u^2$  from ACDM. The obtained analytic expressions were applied to numerical calculations for crystals with face-centred cubic (fcc) and body-centred cubic (bcc) structures and alloys, and applications to copper (Cu), tungsten (W) crystals and tungsten-copper  $W_{93}Cu_{07}$  alloy. Here,  $W_{93}Cu_{07}$  is the alloy with 93% W and 7% ( $\pm 1\%$ ) Cu. Tungsten-copper is a product with very high resistance to heat, hardness, and electrical conductivity. In which,  $W_{93}Cu_{07}$  alloy is used the most.

## 2. Formalism

The non-harmonic EXAFS spectrum is often expressed as [2].

$$\chi(k) = \frac{S_0^2 N}{kR^2} F(k) \exp\left(-\frac{2R}{\lambda(k)}\right) \text{Im}\left(e^{i\phi(k)} \exp\left(2ikr_0 + \sum_n \frac{(2ik)^n}{n!} \sigma^{(n)}(T)\right)\right), \quad (1)$$

where  $S_0^2$  is the intrinsic loss factor due to many electron effects and this quantity characterize for many particles effects,  $N$  is the atomic number of a shell,  $F(k)$  is the atomic backscattering amplitude,  $\phi(k)$  is the total phase shift of photoelectron,  $k$  and  $\lambda$  are the wave number and mean free path of the photoelectron, respectively, and  $\sigma^{(n)}$  ( $n = 1, 2, 3, \dots$ ) are the cumulants and they describe asymmetric components of interactive potential. The latter are due to the thermal average of the function  $e^{-2ikr}$ , in which the asymmetric terms are expanded as a Taylor series around  $R = \langle r \rangle$ , where  $r$  is the instantaneous bond length between absorbing and scattering atoms at temperature  $T$ .

In the non-harmonic approximation and single-bond potential, Eq. (1) is rewritten as [5].

$$\chi(k) = \sum_j \frac{S_0^2 N_j}{kR_j^2} F_j(k) e^{-2\sigma_j^2 k^2} e^{-2R_j/\lambda} \sin[2kR_j + \delta_j(k)]. \quad (2)$$

In the Eq. (2), the exponential function  $DW = 2\sigma_j^2 k^2$  is the Debye–Waller factor (DWF), and the quality  $\sigma_j^2$  is second cumulant or the mean square relative displacement (MSRD) of the bond between two nearest-neighbor atoms [6]. During neutron diffraction or X-ray absorption, the DWF has the similar form of  $DW = (k^2 u_j^2)/2$ . In EXAFS spectra, the DWF is a correlation means to compare the correlation displacement of  $\sigma^2$  for an absorbed and backscattered atoms pair. In contrast, neutron diffraction describes the MSD of an atom.

In atomic oscillation, at temperature  $T$ , two atoms are separated by a distance  $r$  which is described by  $r_j = \hat{\mathfrak{R}}_j^0 (\mathbf{v}_j - \mathbf{v}_0)$ , with  $\hat{\mathfrak{R}}_j^0$  is the component vector and is equal to the unit of the atom  $j$  at balance position,  $\mathbf{v}_j$  is the shift vector of atom  $j$ , and  $\mathbf{v}_0$  is the shift vector of the absorbing atom in the origin position.

Based on Eq. (1), the MSRD  $\sigma^2$  found by averaging the term  $\langle \exp(2ikr_j) \rangle$  [2].

$$\langle \exp(2ikr_j) \rangle \rightarrow \langle \exp[2ik\hat{\mathfrak{R}}_j^0 (\mathbf{v}_j - \mathbf{v}_0)] \rangle = \exp\left(-2\kappa^2 \langle [\hat{\mathfrak{R}}_j^0 (\mathbf{v}_j - \mathbf{v}_0)]^2 \rangle\right). \quad (3)$$

Comparison the Eqs. (1) and (3), for the non-harmonic vibration, we deduce the second cumulant depend on temperature and pressure has the form

$$\sigma_j^2(T, P) = \langle [\hat{\mathfrak{R}}_j^0 (\mathbf{v}_j - \mathbf{v}_0)]^2 \rangle = \langle (\mathbf{v}_j \cdot \hat{\mathfrak{R}}_j^0)^2 \rangle + \langle (\mathbf{v}_0 \cdot \hat{\mathfrak{R}}_j^0)^2 \rangle - 2\langle (\mathbf{v}_0 \cdot \hat{\mathfrak{R}}_j^0) (\mathbf{v}_j \cdot \hat{\mathfrak{R}}_j^0) \rangle. \quad (4)$$

In case  $\mathbf{v}_0 = \mathbf{v}_j$ , quantities  $u_j^2(T, P)$  and  $C_R(T, P)$ , will be written as

$$u_j^2(T, P) = \langle (\mathbf{v}_0 \cdot \hat{\mathfrak{R}}_j^0)^2 \rangle = \langle (\mathbf{v}_j \cdot \hat{\mathfrak{R}}_j^0)^2 \rangle, \quad (5)$$

$$C_R(T, P) = 2\langle (\mathbf{v}_0 \cdot \hat{\mathfrak{R}}_j^0) (\mathbf{v}_j \cdot \hat{\mathfrak{R}}_j^0) \rangle. \quad (6)$$

From Eqs. (4), (5), (6) we have the expression for the relationship between the quantities:

$$C_R(T, P) = 2u_j^2(T, P) - \sigma_j^2(T, P). \quad (7)$$

To determine the quantities in Eq. (7) with the non-harmonic influence, we need to calculate the effective force coefficients (SFCs) of a neighbouring atoms group. The calculation is made by the effectual non-harmonic potential energy, it is a function of the shift  $x$  with the influence of pressure. The non-harmonic potential is written in ACEM (indexed as AE) and ACDM (indexed as AD) [7, 11].

$$U_{eff}^{AE/AD}(x) \approx \frac{1}{2} k_{eff}^{AE/AD} x^2 + k_{3eff}^{AE/AD} x^3, \quad (8)$$

where  $k_{eff}^{AE/AD}$ ,  $k_{3eff}^{AE/AD}$  are the effective SFC and the cubic parameters (CP),  $x = r - r_0$  is the net thermal expansion, and  $r$  is the range of the two atoms at temperature  $T$  and pressure  $P$ , and  $r_0$  is the value of  $r$  in balance position and  $P = 0$  GPa. In Eq. (8), the contrast of quantities  $U_{eff}^{AE}(x)$  and  $U_{eff}^{AD}(x)$  is due to the distinction between the quantities SFCs and CPs.

The effective force constants SFCs and the cubic parameters CP can be received when calculating the effective potential under the influence of both temperature and pressure, with pressures have change magnitudes. We called  $M_1$  and  $M_2$  the mass of absorbed and scattered atoms and considered the approximate mass of the atom pair at the centre of the line joining the two atoms.

In the ACEM, the effective non-harmonic potential  $U_{eff}^{AE}(x, P)$  has the form

$$U_{eff}^{AE}(x, P) = U(x, P) + \sum_{j \neq i} U\left(\frac{\mu}{M_i} x P \hat{\mathfrak{R}}_{12} \cdot \hat{\mathfrak{R}}_{ij}\right), \quad (9)$$

in Eq. (9), quantity  $U(x, P)$  is the powerful potential energy between the absorbing and backscattering atoms under the influence of pressure. The sum of  $i$  runs from 1 to 2 for pairs of absorbing and scattering particles, and the sum of  $j$  runs overall neighbours in a group of atoms. Quantity  $\hat{\mathfrak{R}} = \mathfrak{R}/|\mathfrak{R}|$  is the unit vector and  $\mu = M_1 M_2 / (M_1 + M_2)$  is the reduced mass.

Using ACDM with the potential energy  $U_{eff}^{AD}(x, P)$  is the effective potential energy of a single-particle system. When taking into account only the interactions of  $N$  neighbouring atoms, the effective potential energy  $U_{eff}^{AD}(x, P)$  is

$$U_{eff}^{AD}(x) = \sum_{j=1}^N U(x P \hat{\mathfrak{R}}^0 \cdot \hat{\mathfrak{R}}_j). \quad (10)$$

Using Eqs. (9), (10), and instead of the calculation for the system of equations three-dimensional because of the influence of multi-atoms, we calculate a more simple one-dimensional equation due to using effective interaction potential Morse, with  $N = 12$  for fcc and  $N = 8$  for bcc crystals.

Expand the  $U(x, P)$  to third order, we have

$$U(x, P) = D(e^{-2\varphi x P} - 2e^{-\varphi x P}) \approx D(-1 + \varphi^2 x^2 P^2 - \varphi^3 x^3 P^3 + \dots), \quad (11)$$

in Eq. (11),  $D$  is the dissociation energy and  $1/\varphi$  is width of the potential. For two-component alloy, if the components are denoted by 1 and 2, then we have  $\varphi_{12}$  and  $D_{12}$ , and the values of the quantities are computed in terms of the doping ratio of the alloy [4, 9].

The SFCs are expressed as

$$k_{eff}^{AE/AD} = aD_{12}\varphi_{12}^2, \quad k_{3eff}^{AE/AD} = -bD_{12}\varphi_{12}^3. \quad (12)$$

For the ACD model, the constants  $a = 8$ ;  $b = 3/4$ , in the ACE model  $a = 5$ ;  $b = -5/4$ .

**Table 1.** Quantities  $D_{12}$  and  $\phi_{12}$  and  $\mu$  at pressure 0 GPa compared to experiments [11, 12] and other theory [3].

Quantity/Crystal	$D_{12}$ [eV] (Present)	$D_{12}$ [eV] (Exp. [11, 12])	$D_{12}$ [eV] [3]	$\phi_{12}$ [ $\text{\AA}^{-1}$ ] (Present)	$\phi_{12}$ [ $\text{\AA}^{-1}$ ] (Exp. [11, 12])	$\phi_{12}$ [ $\text{\AA}^{-1}$ ] [3]	$\mu(\times 10^{(-26)})$ [eV/ $\text{\AA}^2\text{s}^{-2}$ ]
Cu–Cu	0.3429	0.3528	0.3426	1.3588	1.4072	1.3591	0.6622
W–W	0.9922	0.9907	0.9915	1.4115	1.4405	1.4122	1.9167
W <sub>93</sub> Cu <sub>07</sub>	0.9467	-	-	1.3982	-	-	1.8289

**Table 2.** Quantities  $k_{\text{eff}}$  and  $k_{3\text{eff}}$  at pressure 0 GPa and compared to other theories [3, 8].

Quantity/ Crystal	$k_{\text{eff}}^{\text{AD}}$ [eV/ $\text{\AA}^2$ ] (Present)	$k_{\text{eff}}^{\text{AD}}$ [eV/ $\text{\AA}^2$ ] [3]	$k_{\text{eff}}^{\text{AE}}$ [eV/ $\text{\AA}^2$ ] (Present)	$k_{\text{eff}}^{\text{AE}}$ [eV/ $\text{\AA}^2$ ] [8]	$k_{3\text{eff}}^{\text{AD}}$ [eV/ $\text{\AA}^3$ ] (Present)	$k_{3\text{eff}}^{\text{AD}}$ [eV/ $\text{\AA}^3$ ] [3]	$k_{3\text{eff}}^{\text{AE}}$ [eV/ $\text{\AA}^3$ ] (Present)	$k_{3\text{eff}}^{\text{AE}}$ [eV/ $\text{\AA}^3$ ] [8]
Cu–Cu	3.1655	3.4931	2.3214	5.0649	0.4748	0.8070	0.7914	0.8831
W–W	9.8840	9.4365	7.2482	7.8143	1.4826	1.4768	2.4710	2.5867
W <sub>93</sub> Cu <sub>07</sub>	9.2537	-	6.7860	-	1.3881	-	2.3134	-

**Table 3.** Quantities  $D_{12}$ ,  $\phi_{12}$ ,  $k_{\text{eff}}$ , and  $k_{3\text{eff}}$  at pressures 0 - 14GPa, application to W<sub>93</sub>Cu<sub>07</sub>.

Pressure[GPa]	$D_{12}$ (eV)	$\phi_{12}$ [ $\text{\AA}^{-1}$ ]	$k_{\text{eff}}^{\text{AE}}$ (eV $\text{\AA}^2$ )	$k_{3\text{eff}}^{\text{AD}}$ (eV $\text{\AA}^2$ )	$k_{3\text{eff}}^{\text{AE}}$ (eV $\text{\AA}^3$ )	$k_{3\text{eff}}^{\text{AD}}$ (eV $\text{\AA}^3$ )
0	0.9467	1.3982	6.7860	9.2537	2.3134	1.3881
5	0.9745	1.2785	6.6332	8.9756	2.2415	1.2426
10	1.3114	1.2168	6.5428	8.6843	2.1902	0.9815
14	1.5830	1.1884	6.3795	8.1782	1.8527	0.9527

To deduce thermodynamic parameters in Eqs. (5), (6), (7), we determined quantities according to the Debye model with all different frequencies, with wavenumber  $q$ . Using the ACD model, we have  $u^2(T; P)$

$$u^2(T, P) = \frac{\hbar c}{2\pi k_{\text{eff}}^{\text{AD}}} \int_0^{\pi/c} 2\sqrt{\frac{2k_{\text{eff}}^{\text{AD}}}{M}} |\sin(qc/2)| \frac{1 + e^{-(\beta\hbar\omega(q))}}{1 - e^{-(\beta\hbar\omega(q))}} dq, \quad \beta = \frac{1}{k_B T}. \quad (13)$$

After substituting  $k_{\text{eff}}^{\text{AD}}$  from Eq. (12) into Eq. (13), quantity  $u^2(T; P)$  as

$$u^2(T, P) = \frac{\hbar c}{16\pi D_{12}\phi_{12}^2} \int_0^{\pi/c} 8\sqrt{\frac{D_{12}\phi_{12}^2}{M}} |\sin(qc/2)| \frac{1 + e^{-(\beta\hbar\omega_{\text{AD}}(q))}}{1 - e^{-(\beta\hbar\omega_{\text{AD}}(q))}} dq, \quad |q| \leq \pi/c. \quad (14)$$

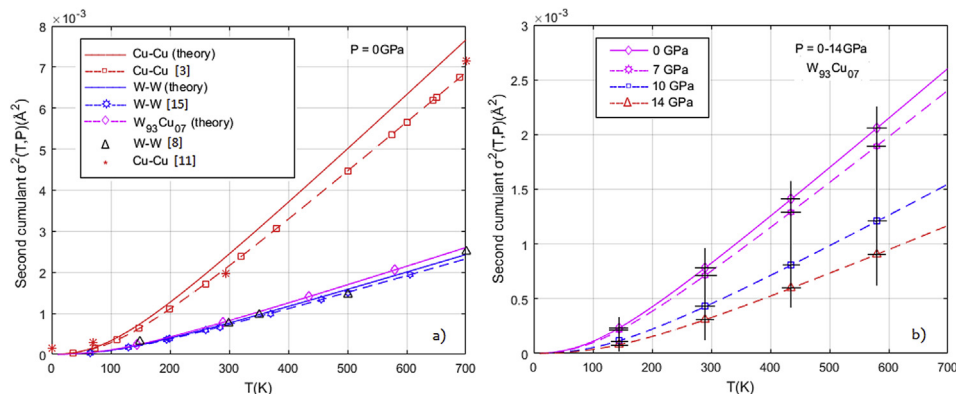
Similar, according to the ACE model, we have the expression of  $\sigma^2(T; P)$

$$\sigma^2(T, P) = \frac{\hbar c}{10\pi D_{12}\phi_{12}^2} \int_0^{\pi/c} \sqrt{\frac{5D_{12}\phi_{12}^2}{\mu} \left(s - \frac{15}{2}\phi_{12}a\right)} \frac{1 + e^{-(\beta\hbar\omega_{\text{AE}}(q))}}{1 - e^{-(\beta\hbar\omega_{\text{AE}}(q))}} dq, \quad |q| \leq \pi/c. \quad (15)$$

with  $s = 5$  for fcc and  $s = 11/3$  for bcc,  $c$  is the net coefficient, the quantities  $q$ ,  $M$ , and  $\mu$  have described above.

From Eqs. (7), (14), and (15) we received  $C_R(T; P)$

$$C_R(T, P) = \frac{\hbar c}{2\pi D_{12}\phi_{12}^2} \left[ \frac{1}{4} \int_0^{\pi/c} 8\sqrt{\frac{D_{12}\phi_{12}^2}{M}} |\sin(qc/2)| \frac{1 + e^{-(\beta\hbar\omega_{\text{AD}}(q))}}{1 - e^{-(\beta\hbar\omega_{\text{AD}}(q))}} dq - \frac{1}{5} \int_0^{\pi/c} \sqrt{\frac{5D_{12}\phi_{12}^2}{\mu} \left(s - \frac{15}{2}\phi_{12}a\right)} \frac{1 + e^{-(\beta\hbar\omega_{\text{AE}}(q))}}{1 - e^{-(\beta\hbar\omega_{\text{AE}}(q))}} dq \right], \quad \beta = \frac{1}{k_B T}, \quad |q| \leq \pi/c. \quad (16)$$

**Figure 1.** Graph depicting second cumulant in terms of  $T$ , application to Cu, W, W<sub>93</sub>Cu<sub>07</sub> at 0 GPa (a), and W<sub>93</sub>Cu<sub>07</sub> alloy up to 14 GPa (b).

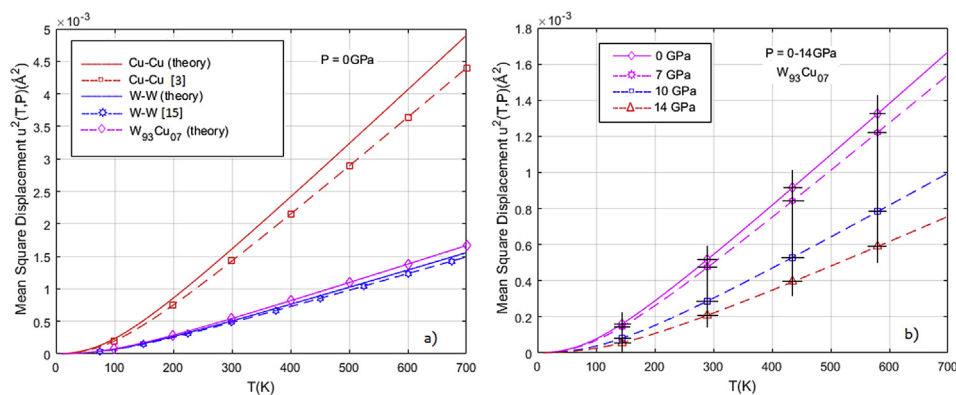


Figure 2. Graph depicting  $u^2$  in terms of  $T$ , application to Cu, W,  $W_{93}Cu_{07}$  at 0 GPa (a), and  $W_{93}Cu_{07}$  alloy up to 14 GPa (b).

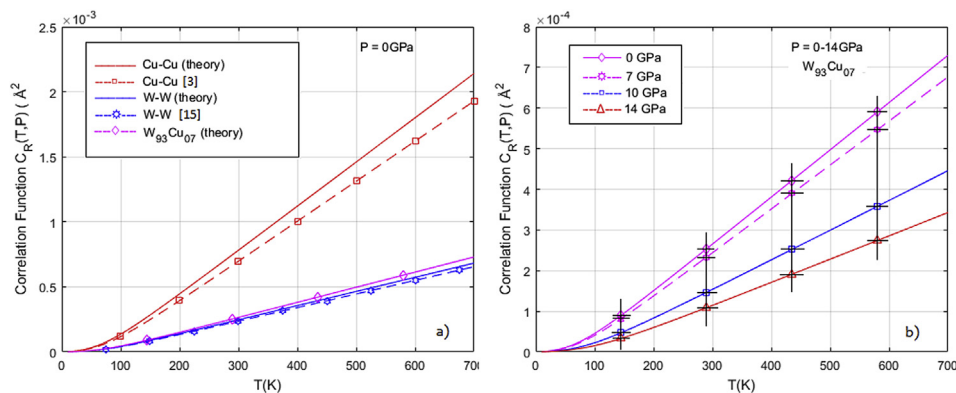


Figure 3. Graph depicting function  $C_R(T, P)$ , application to Cu, W, and  $W_{93}Cu_{07}$  at 0 GPa (a), and  $W_{93}Cu_{07}$  up to 14 GPa (b).

### 3. Results and discussion

Application to calculate for Cu, W crystals and  $W_{93}Cu_{07}$  intermetallic alloy by using Eqs. (14), (15), (16). Theoretical calculation results for the parameters of Morse potential in case unaffected of pressure (0 GPa) are summarized in Table 1, and the SFCs outlined in Table 2. The results in the Tables 1 and 2 have indicated this method is consistent with the measurements from experiments [11, 12] and previous studies [3, 8]. The results of the parameters of Morse potential are listed in Table 3. The elastic force constant and the cubic constant at in case pressure up to 14 GPa application to  $W_{93}Cu_{07}$  alloy have been determined. Substitute the results in Tables 1 and 2 into Eqs. (14), (15), and (16), we received values of quantities  $u^2(T; P)$ ,  $\sigma^2(T;P)$ , and  $C_R(T; P)$ .

Figures 1 and 2 show the dependence on temperature of second cumulant or DWF  $\sigma^2(T; P)$  and MSD  $u^2(T; P)$ , respectively, for Cu, W, and  $W_{93}Cu_{07}$  at pressure 0 GPa (see the graphs in Figures 1a and 2a), and  $W_{93}Cu_{07}$  in the case pressure range from 0GPa to 14GPa (see the graphs in Figures 1b, 2b). In these figures, it can be seen that at high temperatures, the line curves describing quantities  $\sigma^2(T; P)$  and  $u^2(T; P)$  are linearly ratio to the  $T$ , which may apply to classical theory. At temperatures less than, the line curves for Cu, W, and  $W_{93}Cu_{07}$  include the energy of point zero, this is a quantum activation, and  $\sigma^2(T; P)$  is greater than  $u^2(T; P)$  at all temperatures. Thus, the calculated results are suitable because the study used quantum statistical methods, so the results are correct over the whole temperature range. Figures 1b, 2b, for  $W_{93}Cu_{07}$  alloy show that as the pressure increases, the values for  $\sigma^2(T; P)$  and  $u^2(T; P)$  decrease, especially at high temperatures, the values decrease more strongly. In previous studies, the MSD and MSD are only dependent on temperature. Due to thermal oscillations, the pairs of atoms only

displacement around the equilibrium position, at high temperatures, the displacement will be stronger. Nevertheless, when the pressure is increased, it creates a force to limit the thermal vibrations of the atoms and directly affects and reduces the lattice expansion, so the values of  $\sigma^2$  and  $u^2(T; P)$  decrease more strongly at high pressure and temperatures.

Moreover,  $\sigma^2(T)$  has a greater value than  $u^2(T)$ , showing that the damping factor in the EXAFS spectrum of the ACD model is more larger than those of CD model. This difference comes from the choice of the

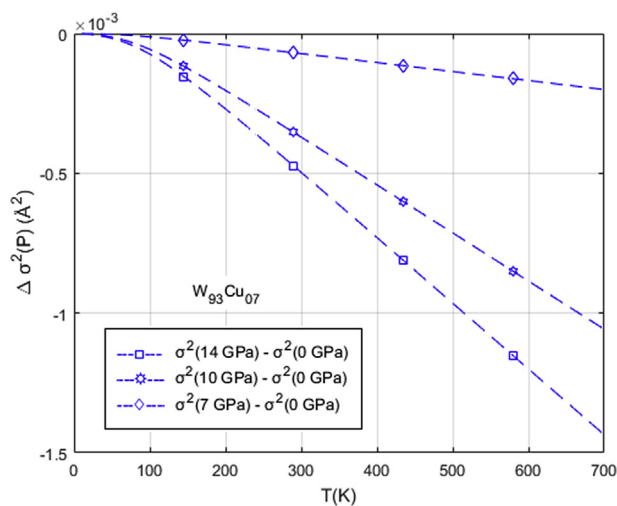


Figure 4. Graph depicting function  $\Delta \sigma^2(P)$ , application to  $W_{93}Cu_{07}$  alloy.

quantity and mass of the atoms in each model. For the ACD model, the number (and hence the mass) of the atom are only 50% of the CD model. Thus, an atom is only as effective as an atom with only half a particle (called quasi-atom).

Figure 3 illustrate the quantity  $C_R(T; P)$ , application to Cu, W, and  $W_{93}Cu_{07}$  at 0 GPa (Fig. 3a), and for  $W_{93}Cu_{07}$  alloy up to 14 GPa (Fig. 3b). Like in Figures 1 and 2, the line curves of  $C_R$  is linearly ratio to  $T$  at significant temperatures and include energy at zero-point at small temperatures. The numerical results of thermodynamic expressions have been built and applied to Cu, W crystals in good agreement with the measurements from the experiment [11, 12] and previous studies [3, 8]. From that can be deduced results application to  $W_{93}Cu_{07}$  alloy is acceptable.

Figures 1b, 2b, 3b describes line curves of the  $\sigma^2(T; P)$ ,  $u^2(T; P)$ , and the  $C_R(T; P)$ , respectively, application to  $W_{93}Cu_{07}$  alloy and influence of pressures in the range from 0 GPa to 14 GPa. As the pressure addition, the curve line of  $W_{93}Cu_{07}$  alloy has formed similar to the curve lines for Cu, W crystals, which means they are linearly ratio to  $T$  at significant temperatures and include energy at zero-point at small temperatures. Simultaneously, as the pressure increases, the values for  $\sigma^2$ ,  $u^2$ , and  $C_R$  decrease, especially at high temperatures and pressure, the values decrease very strongly. As explained above, when the temperature and pressure increase, the lattice expansion and thermal oscillation of the pairs of atoms decrease sharply, so the MSD and MSD decrease very strongly. The bonds of the two types of atoms are more closely due to the bonds energy is higher, making the lattice system much more stable. This one explains why alloy  $W_{93}Cu_{07}$  has a very high hardness and temperature resistance.

Figures 1b, 4 illustrate expressions of the DWF  $\sigma^2(T; P)$  and  $\Delta\sigma^2 = \sigma^2(P) - \sigma^2(0 \text{ GPa})$  have been built and applied to W, Cu crystals and  $W_{93}Cu_{07}$  alloy. The results are compared with experimental measurements [11, 15] and other theories have been published [3, 8, 10]. See these graphs. Our numerical results are in agreement with the results of Dalba et al. and Hung et al. for W and Cu. The DWF curve of  $W_{93}Cu_{07}$  alloy similar to the curve of Cu and W, lower gradually when temperature and pressure increases. At 290K temperature, difference  $\Delta\sigma^2 = \sigma^2(7 \text{ GPa}) - \sigma^2(0 \text{ GPa})$  of  $W_{93}Cu_{07}$  is  $-0.093 \cdot 10^{-3} \text{ \AA}^2$ . At 14 GPa and  $T = 290\text{K}$  difference  $\Delta\sigma^2 = \sigma^2(14 \text{ GPa}) - \sigma^2(0 \text{ GPa})$  is reduced and has a value of  $-0.482 \cdot 10^{-3} \text{ \AA}^2$  (Figure 4). The descent of  $\sigma^2$  graph curve at 700K temperature, at 0GPa and at 14 GPa are, respectively,  $-0.188 \cdot 10^{-3} \text{ \AA}^2$  and  $-1.462 \cdot 10^{-3} \text{ \AA}^2$  (Figure 1b). As a result, the EXAFS spectral amplitude will be reduced. The reason is that when the pressure is increased, the thermal vibrations of the atoms will be limited. Hence the relative displacement of the particles decreases.

#### 4. Conclusions

In this study, the second cumulant and thermodynamic parameters in EXAFS spectra and relationship between parameters due to non-harmonicity have been built by ACEM and ACDM. The numerical calculation have been applied to Cu, W and  $W_{93}Cu_{07}$  alloys. This model has the advantage of using a non-harmonic effective potential, which considers all neighbouring atoms' contributions. The difference between effective SFCs and the number (hence the mass) of particles oscillating in both models gave rise to the difference in thermodynamic properties of the crystal.

The second cumulant, mean square displacement, and correlation function is linearly ratio to  $T$  at significant temperatures and include energy at zero-point at small temperatures, and this is a quantum effect.

The suitable between the numerical results by the method in this work and the data of experiments and computing according to previous studies shows the suitability of the present calculation.

#### Declarations

##### Author contribution statement

Nguyen Ba Duc: Conceived and designed the analysis; Analyzed and interpreted the data; Contributed analysis tools or data; Wrote the paper.

##### Funding statement

This research did not receive any specific grant from funding agencies in the public, commercial, or not-for-profit sectors.

##### Data availability statement

Data included in article/supplementary material/referenced in article.

##### Declaration of interests statement

The authors declare no conflict of interest.

##### Additional information

No additional information is available for this paper.

##### Acknowledgements

The author (N. B. Duc) thanks Tan Trao University, Tuyen Quang, Viet Nam for the support of this study.

#### References

- [1] G. Beni, P.M. Platzman, Temperature and polarization dependence of extended x-ray absorption fine-structure spectra, *Phys. Rev. B* 14 (1976) 1514.
- [2] E.D. Crozier, J.J. Rehr, R. Ingalls, In *X-ray Absorption: Principles, Applications, Techniques of EXAFS, SEXAFS and XANES*, Wiley, New York, 1988, p. 373. Chap. 9.
- [3] G. Dalba, P. Fornasini, R. Grisenti, J. Purans, Sensitivity of X-ray absorption fine structure to thermal expansion, *Phys. Rev. Lett.* 82 (1999) 4240–4243.
- [4] N.B. Duc, V.Q. Tho, Dependence of cumulants and thermodynamic parameters on temperature and doping ratio in extended X-ray absorption fine structure spectra of cubic crystals, *Phys. B Condens. Matter* 55 (2) (2019) 1.
- [5] A.I. Frenkel, J.J. Rehr, Thermal expansion and x-ray-absorption fine-structure cumulants, *Phys. Rev. B* 48 (1993) 585.
- [6] N.V. Hung, J.J. Rehr, Anharmonic correlated Einstein-model Debye-Waller factors, *Phys. Rev. B* 56 (1997) 43.
- [7] N.V. Hung, N.B. Trung, N.B. Duc, D.D. Son, T.S. Tien, Debye-Waller factor and correlation effects in XAFS of cubic crystals, *J. Phys. Sci. Appl.* 4 (1) (2014) 43.
- [8] N.V. Hung, P.Q. Bao, N.B. Duc, L.H. Hung, Debye-Waller Factor and Correlation Effects in XAFS of Cubic Crystals, *Commun. Phys. (Supplement)* (2006) 11.
- [9] B.D. Nguyen, Influence of temperature and pressure on cumulants and thermodynamic parameters of intermetallic alloy based on anharmonic correlated Einstein model in EXAFS, *Phys. Scripta* 5 (7) (2020) 31.
- [10] B.D. Nguyen, V.T. Tho, T.P. Hiep, N.V. Nghia, P.T.H. Minh, V.T.H. Thanh, Investigation of the anharmonic correlation effects by Debye model in X-ray absorption fine structure spectra - application to a two component alloy, *Dalat Univ. Sci.* 10 (3) (2020) 77, 2020.
- [11] M. Okube, A. Yoshiasa, Anharmonic effective pair potentials of group VIII and Lb fcc metals, *J. Synchrotron Radiat.* 8 (2001) 937.
- [12] I.V. Pirog, T.I. Nedoseikina, A.I. Zarubin, A.T. Shuvaev, Anharmonic pair potential study in face-centred-cubic structure metals, *J. Phys. Condens. Matter* 14 (2002) 1825.
- [13] M. Schowalter, A. Rosenauer, J.T. Titantah, D. Lamoen, Computation and parametrization of the temperature dependence of Debye-Waller factors for group IV, III-V and II-VI semiconductors, *Acta Crystallogr. A* 65 (2009) 5.
- [14] J.M. Tranquada, R. Ingalls, Extended x-ray absorption fine-structure study of anharmonicity in CuBr, *Phys. Rev. B* 28 (1983) 3520.
- [15] L. Wenzel, D. Arvanitis, H. Rabus, T. Lederer, K. Baberschke, G. Comelli, Enhanced anharmonicity in the interaction of low-Z adsorbates with metal-surfaces, *Phys. Rev. Lett.* 64 (1990) 1765.